

Sulfonate ester electrolyte regulates Li⁺ desolvation energy to construct high-rate aqueous lithium-ion batterie

Jiajie Zhang,^a Ruixiang Wang,^a Tianyuan Xiao,^a Yan Meng,^b Xiaojuan Chen^{*a}

^aSchool of Chemical Engineering, Sichuan University, Chengdu 610065, Sichuan, China.

^bInstitute of New Energy and Low-Carbon Technology (INELT), Sichuan University, Chengdu 610065, Sichuan, China.

Experimental section:

Chemicals:

Polytetrafluoroethylene emulsion (PTFE, 60wt%), styrene-butadiene rubber emulsion (SBR, 40wt%), lithium carboxymethyl cellulose (CMCLi), lithium bis(fluorosulfonyl)imide (LiFSI, 99.9% purity) was purchased from DoDo Chem Co., Ltd. Ethyl methanesulfonate (EMS, 99% purity), EMC and N-methyl-2-pyrrolidone (NMP, 99.9% purity) were sourced from Adamas Co., Ltd. The LiMn₂O₄ (LMO) and Li₄Ti₅O₁₂ (LTO) powder was purchased from Gansu Rongda New Energy Development Co., Ltd and Hefei Kejing Materials Technology Co., Ltd.

Preparation of cathode and anode

To prepare the LMO cathode, 80 wt% LMO powder, 10 wt% Super P carbon, and 10 wt% PTFE were mixed with a small amount of ethanol and stirred repeatedly in a mortar until a self-supporting electrode structure was formed. The resulting mixture was then rolled onto aluminum foil and dried at 80°C for 5 hours, yielding LMO cathodes with an areal mass loading of approximately 3.7 mg cm⁻². For the LTO cathode, a homogeneous slurry was prepared by dispersing 80 wt% LTO powder, 10 wt% Super P carbon, 6 wt% CMCLi, and 4 wt% SBR binder in water under continuous stirring. The slurry was uniformly coated onto a copper foil substrate using the doctor-blade method and subsequently vacuum-dried at 80°C for 12 hours, resulting in LTO electrodes with an areal mass loading of approximately 2 mg cm⁻². Both types of electrode sheets are cut into circular pieces with a diameter of 14mm.

Battery assembly

The battery assembly process took place within an argon-filled glovebox to ensure the oxygen and water contents remained below 0.1 ppm. LMO/LTO full cells with different electrolytes and celgard 3501 membrane were assembled in CR2032-type coin cells. The battery underwent charge and discharge cycling using a Neware (China) battery testing instrument. The tests were conducted in constant current mode within a voltage range of 1-2.8 V.

Material characterizations

To analyze the interactions among different components in the electrolyte, Fourier transform-infrared spectroscopy (FTIR) was performed on Thermo Scientific Nicolet iS10 spectrometer. The linear sweep voltammetry (LSV) was measured at 0.5 mV s^{-1} using an electrochemical workstation Donghua 7006B (Donghua, China) to obtain the electrochemical window of the electrolyte. To investigate the interfacial chemistry of the LMO and LTO, X-ray photoelectron spectroscopy (XPS, Thermo Fisher Scientific) was performed using monochromatic Al K α radiation (1486.6 eV) as an X-ray source. Time-of-flight secondary ion mass spectrometry (TOF-SIMS) was performed to obtain the depth profile of the LMO electrode on TOF-SIMS M6 (IONTOF GmbH).

Theoretical calculation

Materials Studio tool is applied for the Molecular dynamics (MD) calculations. An amorphous cubic cell with 10 LiFSI, 10 H₂O and 38 EMS (EMC) molecules is constructed for LiFSI: H₂O: EMS (EMC) recipe simulation. Geometry optimization is applied in Forcite package with COMPASS III forcefield assigned. NVT canonical ensemble is chosen for dynamic simulation at 298K with Nose thermostat and 1fs time step for total 1000 ps duration.

Energy density

Selecting a coin battery with an energy of 1001 mWh, the mass of the LTO active material is 3.1 mg, the mass of the LMO active material is 5.735 mg, and the proportion of the electrode active material is 80%. When only taking into account the masses of the positive and negative electrode sheets, the mass energy density is calculated as $1001 \text{ mWh} / [(3.1 \text{ mg} + 5.735 \text{ mg}) * 0.8] = 90.64 \text{ Wh kg}^{-1}$.

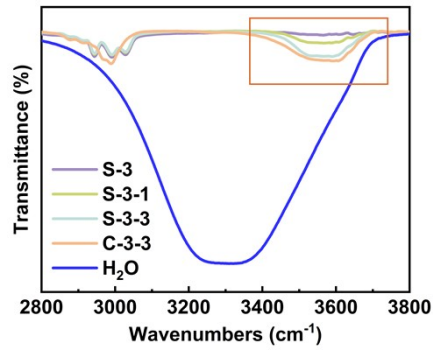


Figure S1. The H-O stretching vibration peaks of S-3, S-3-1, S-3-3, C-3-3 and H₂O.

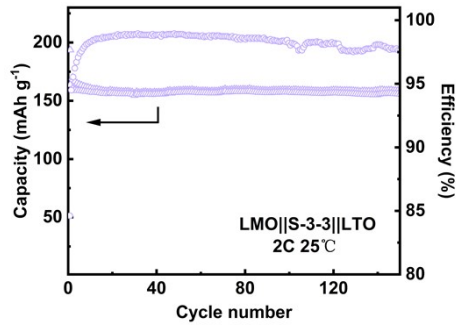


Figure S2. The cycle performance of LMO||S-3-3||LTO at 2C.

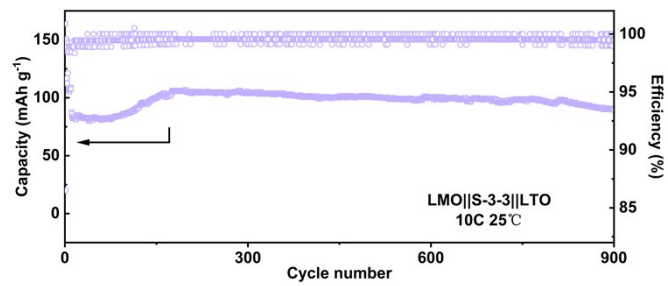


Figure S3. The charging and discharging curve of LMO||S-3-3||LTO. (d) The cycle charge-discharge capacity and CE of LMO||S-3-3||LTO at 10C.

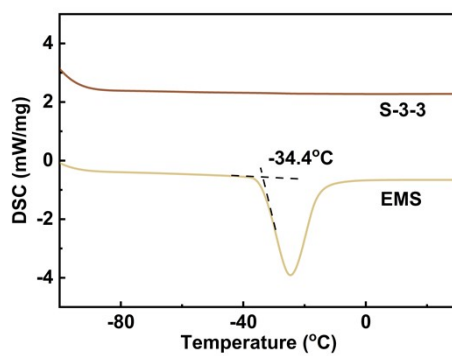


Figure S4. DSC curves of EMS and S-3-3.

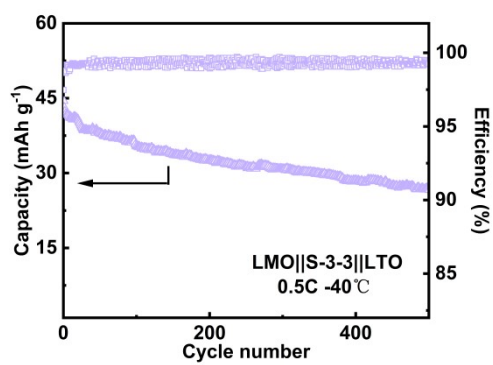


Figure S5. The cycle performance of LMO||S-3-3||LTO at -40°C.

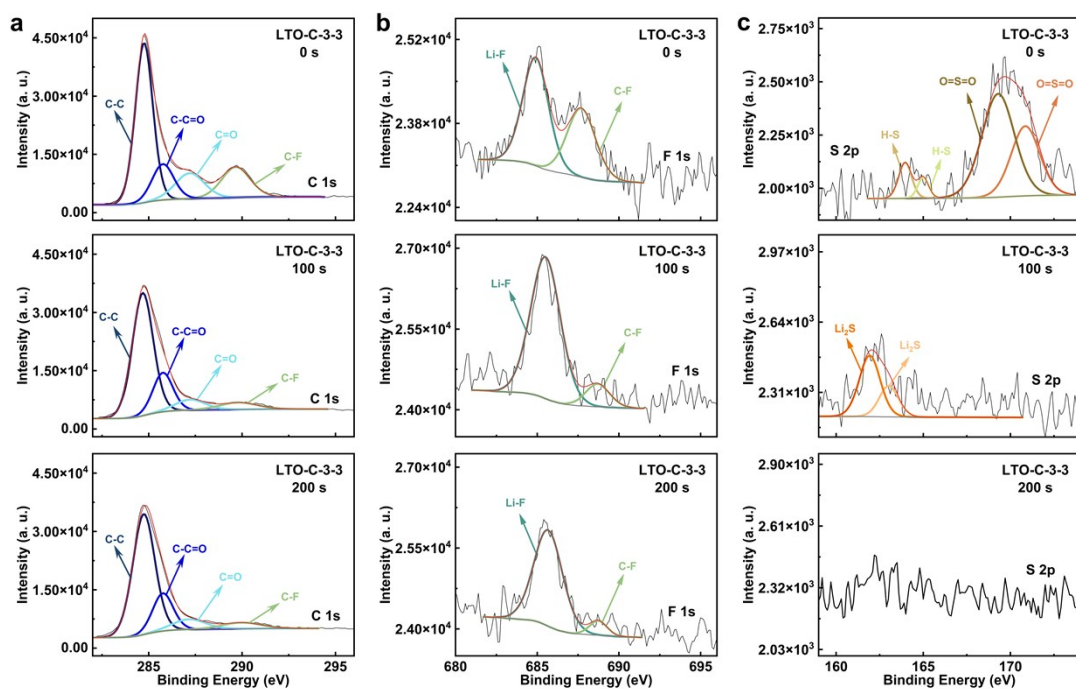


Figure S6. (a) C 1s, (b) F 1s, (c) S 2p spectra of LTO-C-3-3 probed by XPS depth profile.

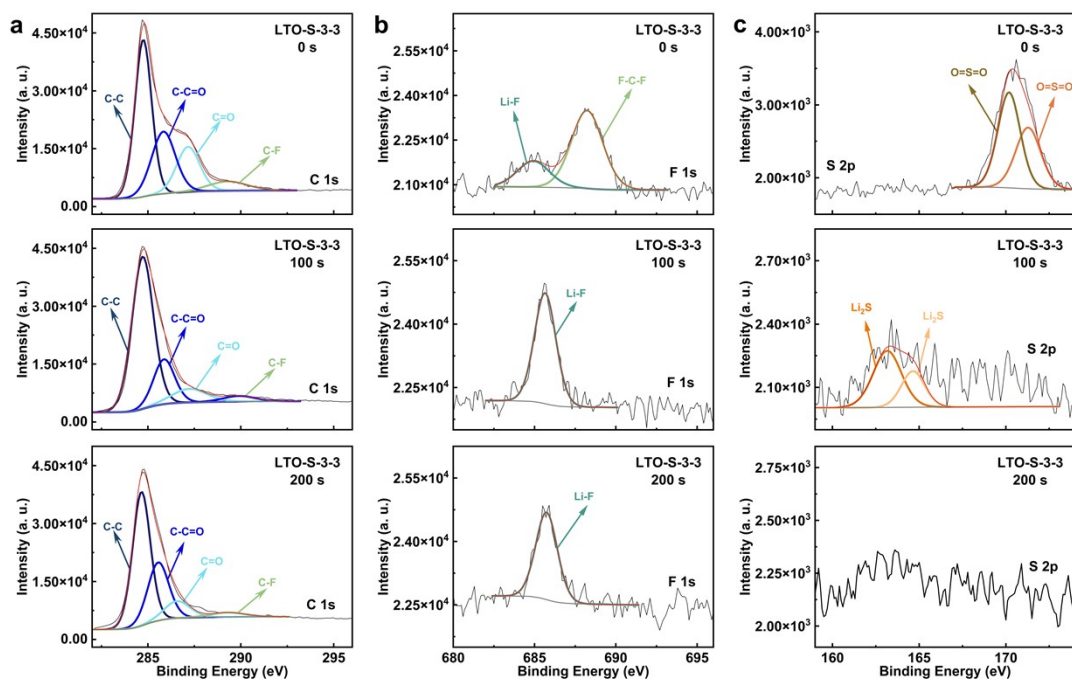


Figure S7. (a) C 1s, (b) F 1s, (c) S 2p spectra of LTO-S-3-3 probed by XPS depth profile.

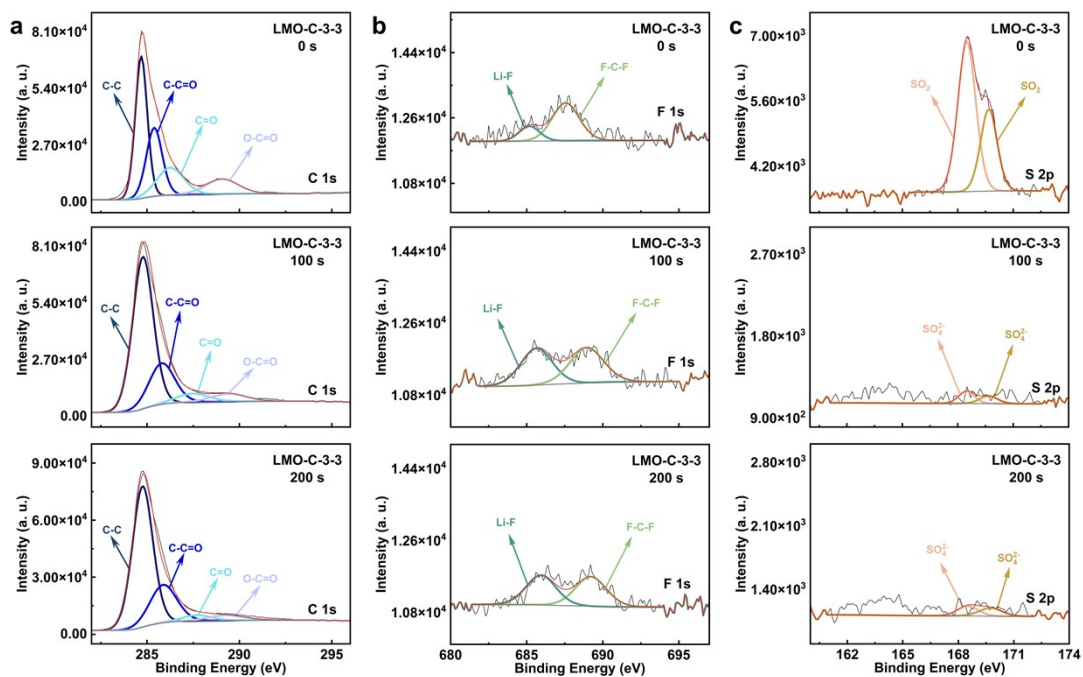


Figure S8. (a) C 1s, (b) F 1s, (c) S 2p spectra of LMO-S-3-3 probed by XPS depth profile.

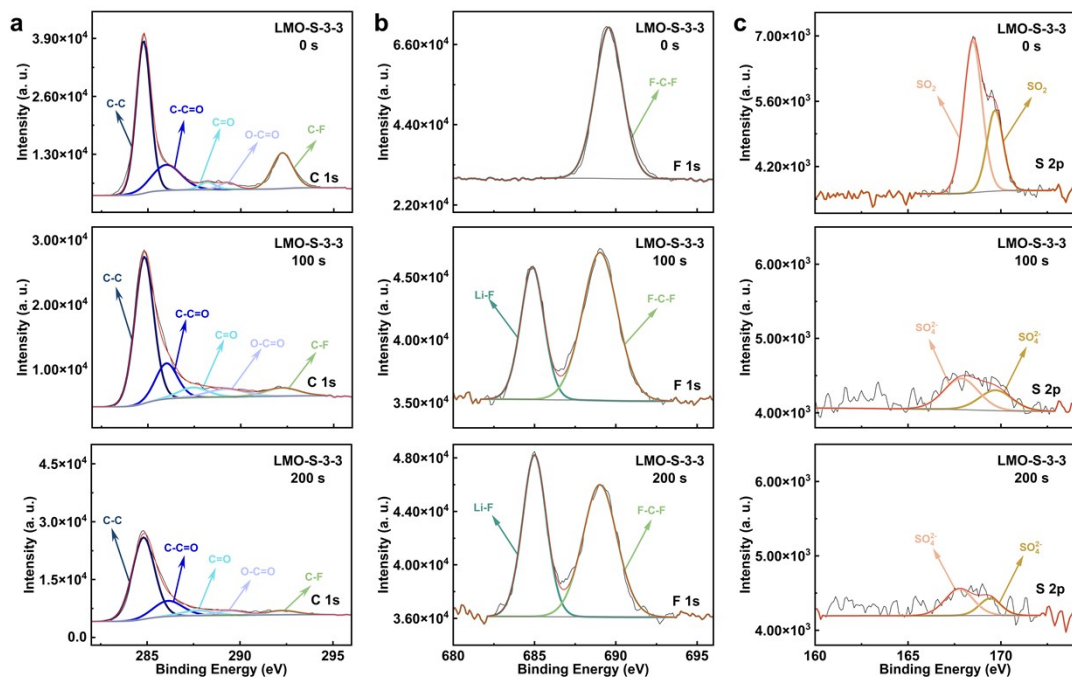


Figure S9. (a) C 1s, (b) F 1s, (c) S 2p spectra of LMO-S-3-3 probed by XPS depth profile.